Instability and Breakup of Model Tear Films

M. Saad Bhamla, Chew Chai, Noelle I. Rabiah, John M. Frostad, and Gerald G. Fuller

Department of Chemical Engineering, Stanford University, Stanford, California, United States

Correspondence: Gerald G. Fuller, Chemical Engineering, Shriram Center, 443 Via Ortega, Room 086, Stanford University, Stanford, CA 94305, USA; ggf@stanford.edu.

Submitted: August 27, 2015
Accepted: January 10, 2016

Citation: Bhamla MS, Chai C, Rabiah NI, Frostad JM, Fuller GG. Instability and breakup of model tear films. *Invest Ophthalmol Vis Sci*. 2016;57:949–958. DOI:10.1167/iovs.15-18064

Purpose. An experimental platform to replicate the human tear film on a contact lens is presented. The influence of interfacial viscoelasticity in stabilizing in vitro model tear films against breakup and dewetting is investigated using this instrument.

Methods. Model tear films consisting of bovine meibomian lipids (meibum) spread on either PBS or artificial tear solution (ATS) are created. The interfacial shear rheology of these films is measured as a function of temperature. The dewetting dynamics of these films is then investigated using the Interfacial Dewetting and Drainage Optical Platform (i-DDrOP) on top of silicone hydrogel (SiHy) contact lenses at 23 and 35°C. The film breakup times are evaluated using two parameters: onset of film breakup, T_{onset} for thick films (~100 μm), and tear breakup times, T_{BU} for thin films (~1 μm). Thin film thinning rates as a result of evaporation are also calculated.

Results. The ATS/meibum films have the largest surface rheology and correspondingly show the largest T_{onset} times at both 23 and 35°C. The parameter T_{BU} is also significantly larger for ATS/meibum ($T_{BU} \sim 40$ seconds) compared with that of ATS and PBS/meibum films ($T_{BU} \sim 30$ seconds) at room temperature. However, at 35°C, all three model tear films exhibit similar $T_{BU} \sim 17$ seconds and average rate of thinning of -4 μm/minute.

Conclusions. Tear film stability is influenced by both surface rheology and evaporation. The in vitro tear breakup times and thinning rates of model tear films at 35°C are in good agreement with in vivo measurements previously reported, highlighting the utility of the i-DDrOP for in vitro tear film breakup research.

Keywords: tear film breakup, meibomian lipids, silicone hydrogel (SiHy) lenses, rheologic properties, dewetting instability

Understanding the physical mechanisms concerning the stability of the natural tear film on our eyes is a challenging problem from an academic, clinical, and industrial perspective.[1–5] Tear film instability can be particularly acute in the presence of a contact lens and results in contact lens–induced dry eyes, a growing epidemic affecting millions of wearers both in the U.S. and worldwide.[6–8] An important component of the tear film is the thin, oily meibomian lipid layer or meibum, secreted by glands located on the upper and lower eyelids.[9] The function of meibum, specifically its role as an evaporation barrier, remains a topic of active debate due to discrepancies between in vivo and in vitro experiments. Animal and human experiments indicate that the presence of meibomian lipids strongly reduces evaporative losses.[10,11] However, in vitro experiments using meibum layers spread on aqueous surfaces have not convincingly reproduced the in vivo results.[12–15] Recent findings have demonstrated that meibomian lipids possess remarkable interfacial viscoelastic properties,[16,17] suggesting an additional role of the meibum layer as a stabilizing agent against tear-film breakup.[18] The linkages of this lipid layer to tear film stability have been recognized through in vivo clinical observations of tear breakup time (TBUT) of healthy and diseased patients,[19–23] as well as through in vitro rheologic measurements on a Langmuir trough.[24] However, experiments that connect these basic structural and rheologic findings to tear film stability are still needed. Previous work has described the ability of meibum layers to form stabilizing films on flat silicon wafer substrates.[25] However, these experiments need to be treated with caution as they are conducted at room temperature, which is below the melting transition of meibum and involved water as the subphase. Consequently, these results did not accurately mimic the conditions of the eye. Thus, the design of an in vitro platform that replicates the human tear film remains an unmet, yet important challenge.

In this work, we report the dewetting dynamics of in vitro tear films consisting of artificial tear solutions (ATS) supporting meibum overlayers on silicone hydrogel (SiHy) contact lens substrates. These are performed at physiological temperatures, using a newly developed instrument (Interfacial Dewetting and Drainage Optical Platform [i-DDrOP]; Stanford University, Stanford, CA, USA). The surface rheology of both the aqueous ATS subphase and the insoluble meibomian layer can be controlled since the device is integrated into a mini-Langmuir trough. We demonstrate a simple way of identifying thin films on the order of ~1 μm appropriate to the thickness of the in vivo prelens tear film (PLTF). We measure the breakup times (T_{BU}) of our thin films and compare them to the in vivo measured noninvasive breakup times (NI-BUT). We also measure the tear film thinning rates for the model tear films and comment on the role of evaporation. Our work thus constitutes a simple, bench-top instrument that serves to replicate the surface of the eye with potential opportunities in fundamental investigations of tear film stability and design of artificial tear therapeutic solutions.

Materials and Methods

SiHy Lenses

In all the experiments conducted in this study, a single type of commercial SiHy lens was used (senofilcon A; Johnson & Johnson, Jacksonville, FL, USA). A low dioptric power of –0.50 was used to avoid thickness undulations across the lens surface. As disclosed by the manufacturer, the senofilcon A lenses are silicone hydrogels with 38% water content and 62% principal monomers that include monofunctional polydimethylsiloxane, N,N-dimethylacrylamide, hydroxyethyl methacrylate, tetraethyleneglycol dimethacrylate and polyvinyl pyrrolidone.

Lens Cleaning Protocol

The lenses were obtained in commercial blister-packs containing propriety surfactant solution that can impact the dewetting experiments. Thus, prior to any experiments, the blister-pack solution was leached out using the following in-house protocol. Each well of a 12-well plate (Corning, Inc., Corning, NY, USA) was filled with 5 mL of PBS (Gibco Life Technologies, Grand Island, NY, USA). After introduction of the lenses to the PBS-filled wells, they were gently agitated for 20 minutes and then transferred to wells containing fresh PBS for another 20 minutes of agitation. Finally, the lenses are transferred to wells containing fresh PBS and agitated overnight. Before using the lenses the following day, the lenses were gently rinsed in fresh PBS to remove any final traces of blister-pack surfactants. The lenses were handled only with silicone-tipped Nylon mini-tweezers.

Model In Vitro Tear Film Solutions

Artificial Tear Solution. We used 1.90 mg mL^{-1} lysozyme (L6876); 0.15 mg mL^{-1} mucin from bovine submaxillary glands (M3895); 5% by volume fetal bovine serum (12003C); and PBS solution (Gibco). All the chemicals were acquired from Sigma-Aldrich Corp. (St. Louis, MO, USA). The artificial tear solution was prepared fresh for each experiment and used within a few hours of preparation to prevent degradation.

The specific concentrations for each chemical were chosen to mimic the protein-rich aqueous phase of the human tear film based on values published in literature.[26,27] The measured surface pressure of the fresh ATS was $\Pi = 15 \pm 2$ mN m^{-1}, where the surface pressure is defined as $\Pi = \gamma_0 - \gamma$, where γ_0 is the surface tension for the bare surface (72.8 mN m^{-1} for PBS), and γ is the surface tension in the presence of surfactant molecules. The bulk shear viscosity of ATS was measured using a rheometer and found to be shear thinning. The bulk viscosity decreased from 2 to 1 mPa as frequency was increased from 1 to 50 Hz, at both 23 and 35°C.

Meibomian Lipids (Meibum). Bovine meibomian lipids were employed as models for the lipid-rich phase of the human tear film, as they are structurally and rheologically similar to human meibum.[16] Lipids were harvested from cow eyelids obtained from a local abattoir observing animal ethics guidelines. The eyelids were transported fresh on the same day to the laboratory in sealed bags. Upon arrival, the eyelids were incubated at 37 ± 2°C to ease the flow of lipids from the meibomian glands. The lipids were squeezed out by applying force on the eyelid margins following the protocol of Nicolaides et al.[28] Meibum from multiple eyelids was pooled together and collected on a glass coverslip using a spatula, which was then stored in an amber jar at –20°C until use. Prior to experimental use, the meibomian lipids were dissolved in chloroform (Sigma-Aldrich Corp.) to a concentration of 1 mg mL^{-1}.

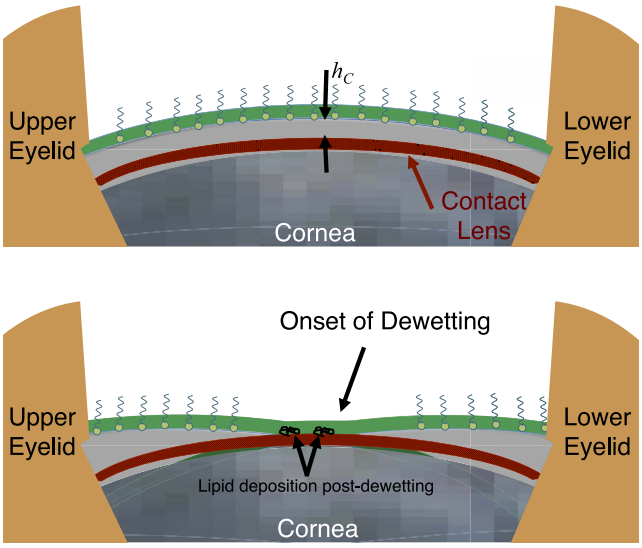

Figure 1. Schematic (not to scale) illustrating the drainage and dewetting dynamics of PLTF in the presence of a SiHy contact lens on our eyes.

Interfacial Shear Rheology

A commercial interfacial shear rheometer (KSV NIMA Ltd., Helsinki, Finland) was employed to measure the interfacial shear rheology of the tear film solutions.[29,30] For measurements of ATS, the trough was filled with freshly prepared solution and measurements were taken every 10 seconds. For films with PBS/meibum, the trough was filled with PBS and meibomian lipids were spread dropwise at the air-PBS interface using a microliter Hamilton syringe. The barriers were compressed until a surface pressure of $\Pi = 16$ mN m^{-1} was reached. For the ATS/meibum measurements, ATS was filled into the trough and heated to 37°C and meibum added dropwise at the air-ATS interface. This ensured uniform spreading of meibum. Temperature sweeps were conducted by transitioning the subphase between 23 to 35°C (ATS [no film] and PBS/meibum) or 26 to 35°C (ATS/meibum). All the measurements were conducted at a frequency of 1 Hz at a maximum applied strain of 0.5%.

Experimental Setup: i-DDrOP

The dewetting experiments in this report were conducted using the bench-top instrument developed in the Fuller Laboratory at Stanford University. The instrument is designed to experimentally model the simplified tear film processes of drainage and dewetting occurring during a blink-cycle as illustrated in Figure 1. Postblink, the prelens tear film undergoes drainage, diminishing in thickness under the combined effects of evaporation, gravity, capillary, and osmotic stresses.[30] Once the tear film thickness is sufficiently diminished locally, dewetting instabilities occur, resulting in breakup or dewetting of the tear film on the anterior surface of the lens.[31] Dewetting of the tear film may also transfer the lipid onto the underlying lens substrate, resulting in fouling of the lens surface. This fouling can modify the lens surface wettability[32] with acute ophthalmologic consequences for the lens wearer, including inflammatory disorders, reduced vision, and symptoms of dry eye.[2,8,33]

A photograph and schematic of the instrument is seen in Figure 2. The device integrates a customized mini-Langmuir trough that allows spreading of insoluble lipid layers on top of

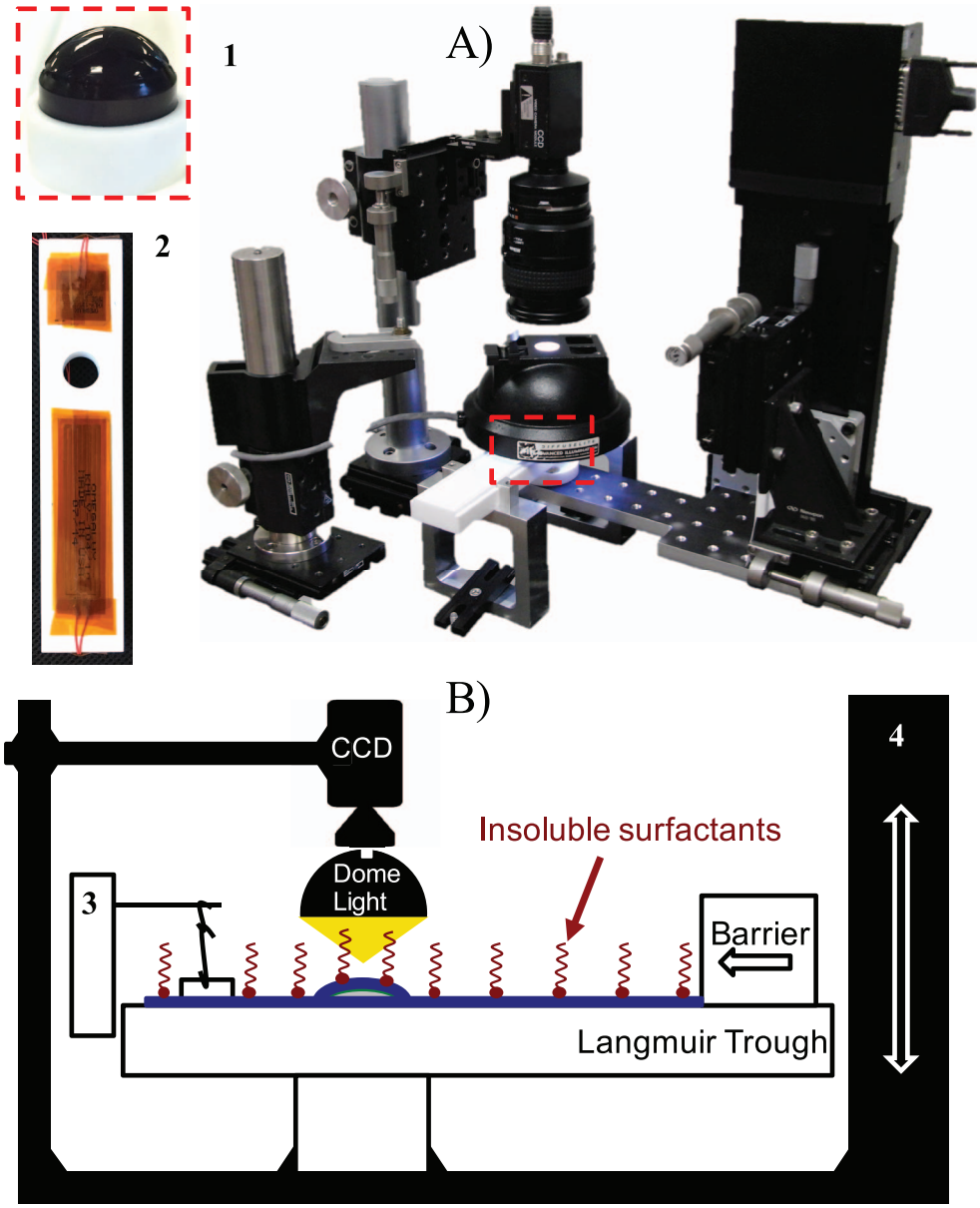

FIGURE 2. Photograph (**A**) and schematic (**B**) of the bench-top instrument (Stanford University). A contact lens is supported on an anodized aluminum dome with matching base curvature radius (see *inset 1*). The dome can travel up and down through a circular cavity in the customized mini-Langmuir trough (see *inset 2*). The base of the Langmuir trough has aluminum blocks with flexible heating elements attached to them for temperature control (*inset 2*). With the lens initially submerged in the liquid-filled trough, meibomian lipids are spread at the air-liquid interface and compressed with a Delrin barrier to the desired surface pressure, which is monitored using a surface pressure sensor (*inset 3*). The temperature of the air-liquid interface is simultaneously monitored using a digital thermocouple probe (not shown). The lens is then elevated through the air-liquid interface using a computer controlled motorized stage (*inset 4*), capturing a stratified layer of aqueous film laden with meibomian lipids. The dewetting dynamics of this thin film on the contact lens surface are then captured using a color camera illuminated by a diffused, dome light source.

an aqueous subphase at controlled surface pressures. This trough is equipped with a lens-supporting dome and heating capability (see insets 1, 2 of Fig. 2). The dome has a radius of curvature (R = 8.6 mm) that matches the base curve of commercial SiHy lenses. This enables contact lenses to remain secure in place by lubrication forces similar to on-eye placement, eliminating the need for any mechanical securement devices in our instrument.

The heating module consists of polyimide flexible heating elements (KHLV-101/10-P; Omega Engineering, Stamford, CT, USA) attached to ~5-mm thick aluminum blocks inserted into the base of the trough. A K-type thermocouple (TJ36-CASS, Omega Engineering) is inserted into the subphase solution to continuously monitor the temperature using a temperature control box, with a sensitivity of ±0.1°C.

The trough is kept stationary while the dome is mounted on a computer-controlled motorized platform (inset 4, Fig. 2B, ILS150HA; Newport Corp., Irvine, CA, USA). The stage can elevate the dome (supporting a SiHy contact lens) from an initial position slightly below the interface at a range of speeds (0.001–25 mm s^{-1}). For all the experiments reported, the lenses were elevated at a speed of 10 mm s^{-1} for a distance of ~3 mm from its starting position, exposing a spherical cap ~10 mm in diameter.

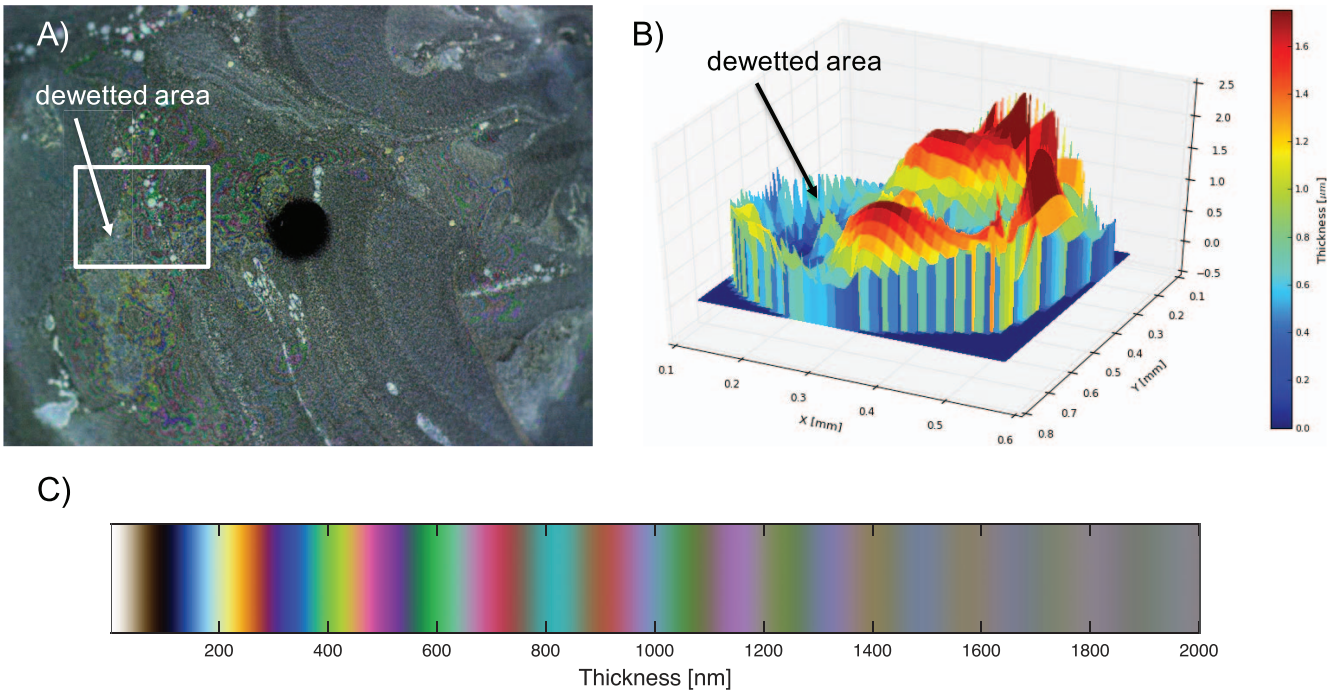

FIGURE 3. (**A**) Snapshot at $t = 142.9$ seconds during dewetting of ATS/meibum film at 35°C. (**B**) A 3D surface contour map is generated for the area enclosed by the *white square* on the left image. The contour is only shown to highlight the rich topologic features and the thickness range that can be interpreted from the color fringes. (**C**) Theoretical color spectrum that correlates interference colors to film thicknesses.

A typical dewetting experiment is conducted as follows. The trough is filled with the aqueous subphase (PBS or ATS) and the lens is submerged in the solution. For the meibum experiments, ~30 μL of lipid solution is deposited at the air-liquid interface and compressed manually using a Delrin barrier. The surface pressure is monitored using a Wilhelmy balance (inset 3, Fig. 2B, KSV NIMA; Biolin Scientific Holding AB, Stockholm, Sweden). The lens is then elevated, resulting in the capture of a stratified film consisting of a meibum-laden aqueous layer on the lens substrate.

A white LED dome light (DL194; Advanced Illumination, Rochester, VT, USA) is used in conjunction with a color charge-coupled device (CCD) camera (DCU223; Thorlabs, Inc., Newton, NJ, USA) to acquire high quality images of dewetting films on the SiHy substrates. The black anodization of the dome supporting the lens facilitates the acquisition of high-contrast images of the lens surfaces undergoing dewetting. In this study, we conduct measurements at room temperature (23°C) and physiologically relevant temperature (35°C).

White Light Interferometry Analysis

The processes of drainage and dewetting on contact lenses produce complex, time-dependent thickness variations (see Figure 3A). Obtaining white light interferometry images from the i-DDrOP (Stanford University) is accomplished through video recordings of the model tear films using a combination of a high resolution color CCD camera and a white LED light source (400–760 nm), as described in the previous section. The resulting high-resolution color videos are then translated into thickness profiles using software developed in-house. This is accomplished by comparing the color value of each pixel (RGB), and its progression in time, with a theoretical color map shown in Figure 3C (calibration data is shown in Supplementary Fig. S3). The color interferometry is illustrated with an example in Figure 3 that highlights a dewetting ATS/meibum film. The color interference patterns can also be used to generate 3-dimensional (3D) surface contours of the thin film as shown in Figure 3B. For the current analysis in this report, we use the color fringes to determine a film thickness of 1.0 ± 0.3 μm and then follow the decay in thickness, which enables us to estimate the breakup times and the thinning rates for the thin films as described in the next sections.

Breakup Times (T_{onset} and T_{BU}) and Evaporation Rates

To convert the qualitative dewetting videos (see Supplementary Material) into quantifiable information that is useful for comparative analysis, we binarize the captured RGB videos into black and white videos using a computing environment (MATLAB; MathWorks, Natick, MA, USA). This enables digitization of the area, and a plot of the normalized wet area to total area as a function of time is shown in Figure 4. This plot highlights: the drainage regime, in which the area-ratio remains unity; the dewetting regime, in which the area-ratio decreases to zero; and T_{onset}, which denotes the onset of the dewetting instability and demarcates the transition between the two regimes. The latter T_{onset} parameter serves as a measure of the stability of the thin liquid films and is utilized as a parameter to compare the stabilization influences of different model tear films.

Additionally, for the model tear films, a second parameter is calculated, $T_{BU} = T_{onset} - T_{fringe}$, where T_{fringe} is the time at which color interference patterns indicate a film thickness of 1.0 ± 0.3 μm. This thickness was chosen since it is appropriate to values normally associated with the PLTF thicknesses[34,35] and well within the confidence range of our color interferometer.

It is important to note that the initially captured model tear films have an initial thickness (~100 μm) and drain predominantly due to gravitational forces, since the volumetric flux is

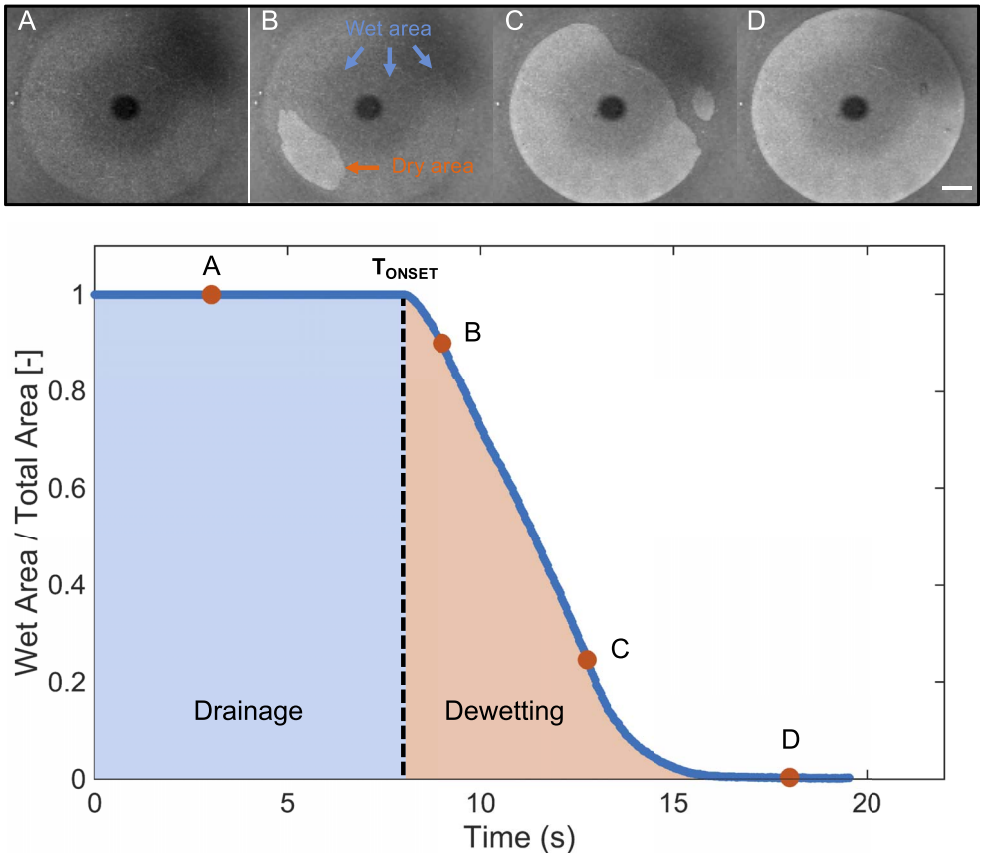

FIGURE 4. A characteristic dewetting plot for PBS on a SiHy contact lens indicating the drainage and dewetting regimes. The curve is obtained by quantifying the fractional wet area to total area ratio as a function of time. The images above are snapshots from the recorded video at: (**A**) $t = 4.0$ seconds, (**B**) $t = 9.0$ seconds, (**C**) $t = 12.8$ seconds, and (**D**) $t = 18.0$ seconds. *Scale bar*: represents 1 mm.

proportional to the cube of the thickness ($Q \propto h^3$).[30] However, once the color fringes appear, the films are ~1 μm thick and flow due to gravity would be reduced by a factor of 10^6, and thus flows will be dominated by capillarity forces and evaporation. To calculate the rates of evaporation (dh/dt), we measure the thickness as a function of time using the color scale in Figure 3. These curves are fitted to a linear relationship and the slopes indicate the rate of thinning due to evaporation.

RESULTS

Surface Shear Rheology

The surface shear moduli as functions of temperature for the three model tear films are shown in Figure 5. In this figure, the filled symbols represent the elastic modulus G_s' and the open symbols represent the viscous modulus G_s''. The viscoelasticity of meibum deposited on top of PBS is shown in green squares at $\Pi = 16$ mN m^{-1}. At 23°C for meibum, $G_s' > G_s''$ and the film has more solid-like characteristics. However, upon heating, both G_s' and G_s'' decrease by more than two-orders of magnitude as the temperature increases from 23 to 37°C. At 34°C, only the G_s'' is measured ($G_s' = 0$), indicating more liquid-like characteristics before the sensitivity of the rheometer (1.01 mN m^{-1}) is reached.

The artificial tear solution layer exhibits significant interfacial viscoelasticity within the temperature range measured (blue circles). Between 23 and 37°C, $G_s' > G_s''$ and both moduli decrease by only a factor of 3, unlike the dramatic decrease seen for PBS/meibum. At 23°C, the G_s' for ATS is 4.81 mN m^{-1}, slightly lower than that of PBS/meibum.

In the case of ATS/meibum (red triangles), the film is highly viscoelastic ($G_s' > G_s''$) over the temperature range measured.

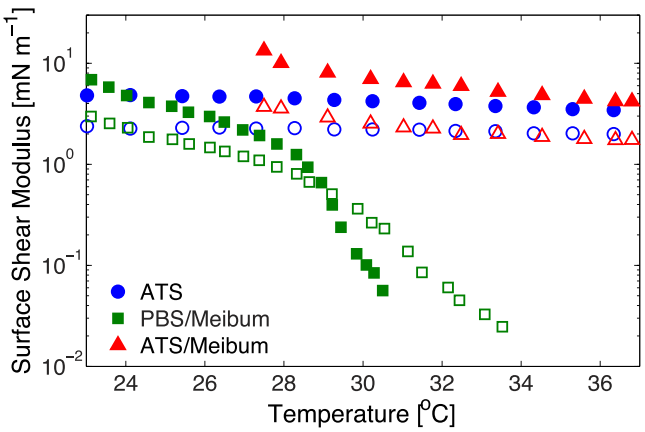

FIGURE 5. Interfacial shear moduli measured as a function of temperature for model tear films at a frequency of 1 Hz. All three solutions are at $\Pi = 15 \pm 2$ mN m^{-1}. Temperature sweeps were conducted by transitioning the subphase between 23 to 35°C (ATS [no film] and PBS/meibum) or 26 to 35°C (ATS/meibum). The *filled symbols* represent the elastic shear modulus G_s' and the *open symbols* represent the viscous shear modulus G_s''. *Error bars* are within the size of the data points.

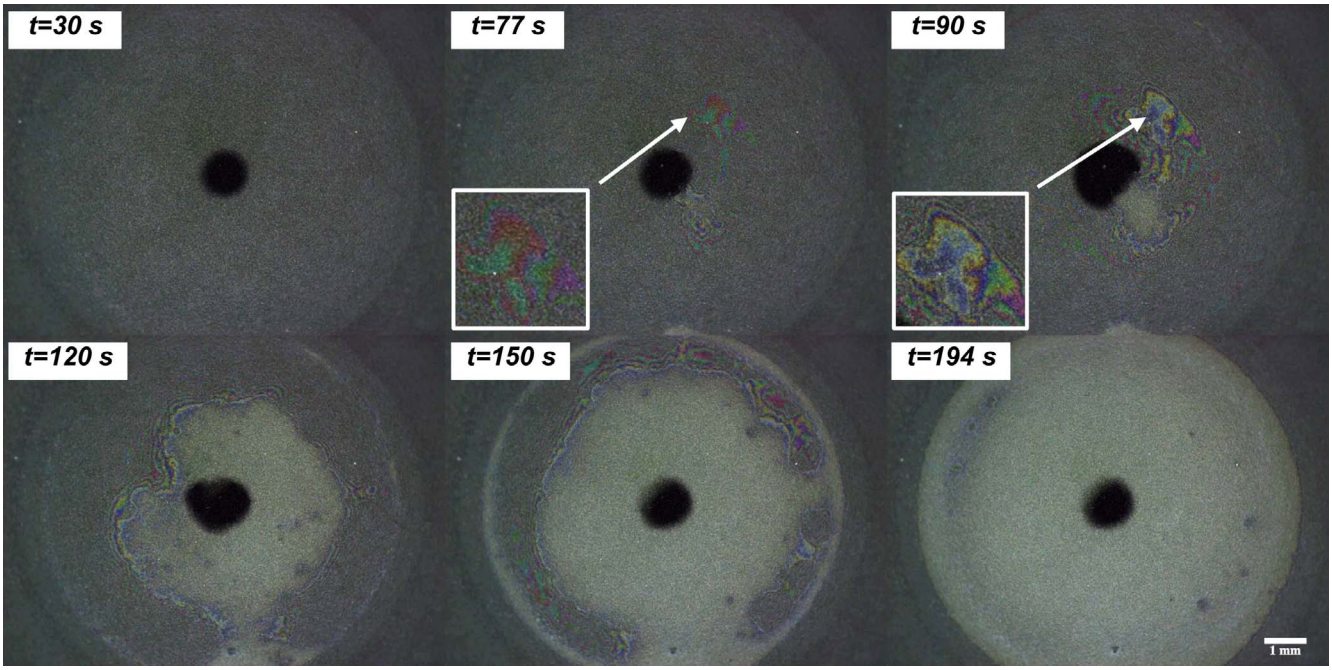

FIGURE 6. Time snapshots of an ATS film dewetting on a SiHy lens at 35°C. In this and subsequent figures, the legend at the *top left* indicates the time, started when the lens was elevated through the air-liquid interface. The *black circle* in the center of each frame is an optical reflection due to the camera and not a physical marking on the SiHy lens. Inserts are zoomed-in areas at locations indicated by the *white arrows*. *Top row*: after ~70 seconds, the film reaches $h_C \sim 1$ μm and thin film color interference bands are observed. *Bottom row*: eventually the films dewet exposing the underlying dry SiHy lens surface. *Scale*: 1 mm.

The moduli reach the maximum measurable limit of the rheometer at 26°C.

Dewetting Dynamics of Model Tear Films

PBS. The dewetting dynamics of thin liquid films on SiHy lenses are first illustrated using a simple control experiment utilizing PBS as the subphase liquid. Snapshots at different time-points are shown in Figures 4A through 4D. The images provide a bird's eye view of the exposed lens substrate and the black spot in the center is the reflection of the camera. We captured a PBS-liquid film by elevating the SiHy lens through the air-PBS interface. At short times ($t < 10$ seconds), the film drains due to gravity as described previously.[30] Once the film reaches a critical thickness, dewetting ensues from a nucleation site and the liquid film recedes, exposing the underlying dry SiHy substrate. This dewetting process occurs in less than 20 seconds and the whole process can be observed clearly in the attached movie in the Supporting Information section.

ATS. Artificial tear solution films exhibit qualitatively and quantitatively distinct behavior in comparison with PBS films as shown in Figure 6. The frames show six snapshots through the dewetting stages of an ATS film at 35°C with the time stamps on the top-left corner. The first frame shows the fully wetted ATS film at 30 seconds still undergoing slow drainage. This is unlike the PBS film that completely dewets in <20 seconds. Around ~70 seconds, color interference patterns start to appear on the ATS film (see inset of frame 2 in Fig. 6). These interference patterns appear in thin films (<2 μm) due to constructive and destructive interference of light. The colors represent thickness values as shown in Figure 3.

Within tens of seconds, the color fringes change, indicating local thinning of the ATS film until a critical thickness is reached, after which dewetting initiates. The color fringes and consequent dewetting patches are initially observed closer to the apex, followed by radial increase in the dry patch area, until the entire exposed SiHy surface is dry. The entire dewetting process takes ~3 minutes.

PBS/Meibum. The dewetting process for meibum films on PBS layers (PBS/meibum) at 35°C and $\Pi = 16$ mN m^{-1} is shown in Figure 7. The heterogenous polydomain structure of meibum is quite evident in the first image as meibum consists of a rich mixture of lipids (both polar and nonpolar) that form domains of lipid aggregates and has been observed by us and others in the past.[24,36]

Compared with a bare PBS film, the PBS/meibum film is quite stable. The color fringes start to appear at ~90 seconds across the film surface. Furthermore, in contrast to the ATS film, the PBS/meibum film locally thins at multiple sites at numerous radial positions. Consequent nucleation and dewetting proceeds at these locations as the liquid film recedes. Past work has shown that the dewetting mechanism results in transfer of the insoluble lipids at the moving contact line and subsequent fouling of the SiHy surface, ultimately affecting the lens wettability.[31,32] The whole dewetting process takes ~5 minutes, leaving behind a dry SiHy surface that is fouled with a meibum layer.

ATS/Meibum. The dewetting process for an ATS/meibum film at 35°C is shown in Figure 8. Similar to PBS/meibum, the interface appears heterogenous and the dewetting process proceeds through multiple nucleation sites. However, the ATS/meibum film is more stable as seen by the appearance of the fringes at ~135 seconds. The entire process for ATS/meibum takes ~5 minutes.

Onset of Dewetting, T_{onset}

A summary of the onset of dewetting instability times (T_{onset}) for all the model tear films at 23 and 35°C is shown in Figure 9. The exact values, including the standard deviations, are presented in the accompanying Table for easy comparison.

The bare PBS films are the least stable with the shortest onset of dewetting times of 14.2 ± 4.7 and 18.3 ± 2.3 seconds

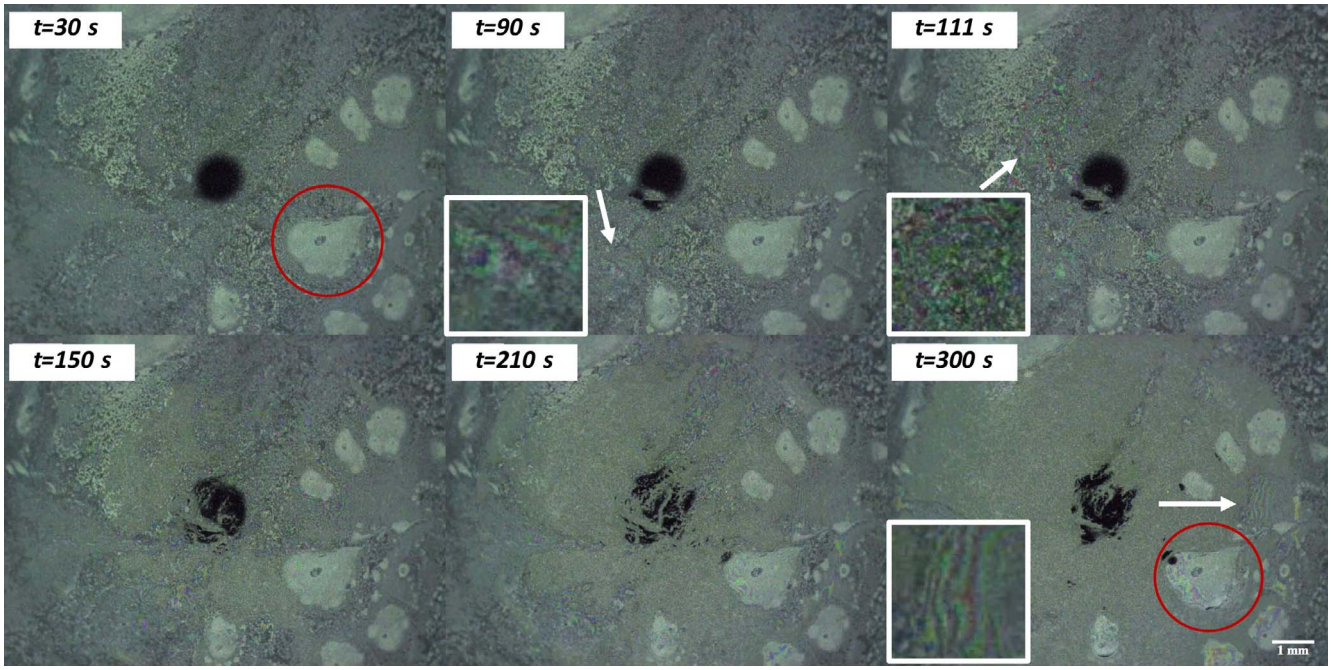

FIGURE 7. Time snapshots of a PBS/meibum film dewetting on a SiHy lens at 35°C. Inserts are zoomed in areas at locations indicated by the *white arrows*. The film PBS/meibum dewets through nucleation at random sites located all over the lens surface. *Scale*: 1 mm.

at 23 and 35°C, respectively. For bare ATS films, the onset times increase to 125.5 ± 6.9 and 91.4 ± 6.4 seconds at 23 and 35°C, respectively.

The presence of meibum in stabilizing the film against breakup is seen clearly as the onset time for PBS/meibum is increased to 147.2 ± 33.5 and 113.7 ± 24.3 seconds at 23 and 35°C, respectively. Thus, compared with the bare ATS films, PBS/meibum films are stable by almost a minute longer. Finally, the combination of ATS/meibum results in the largest onset times of 194.4 ± 52.9 and 133.9 ± 18.3 seconds at 23 and 35°C, respectively.

Breakup Time, T_{BU}

The breakup times $T_{BU} = T_{onset} - T_{fringes}$ are shown in Figure 10. This is not applicable to the bare PBS film as they initiate dewetting at $h_c > 2$ μm and no color fringes are observed. Using this definition, we find that all three model tear films

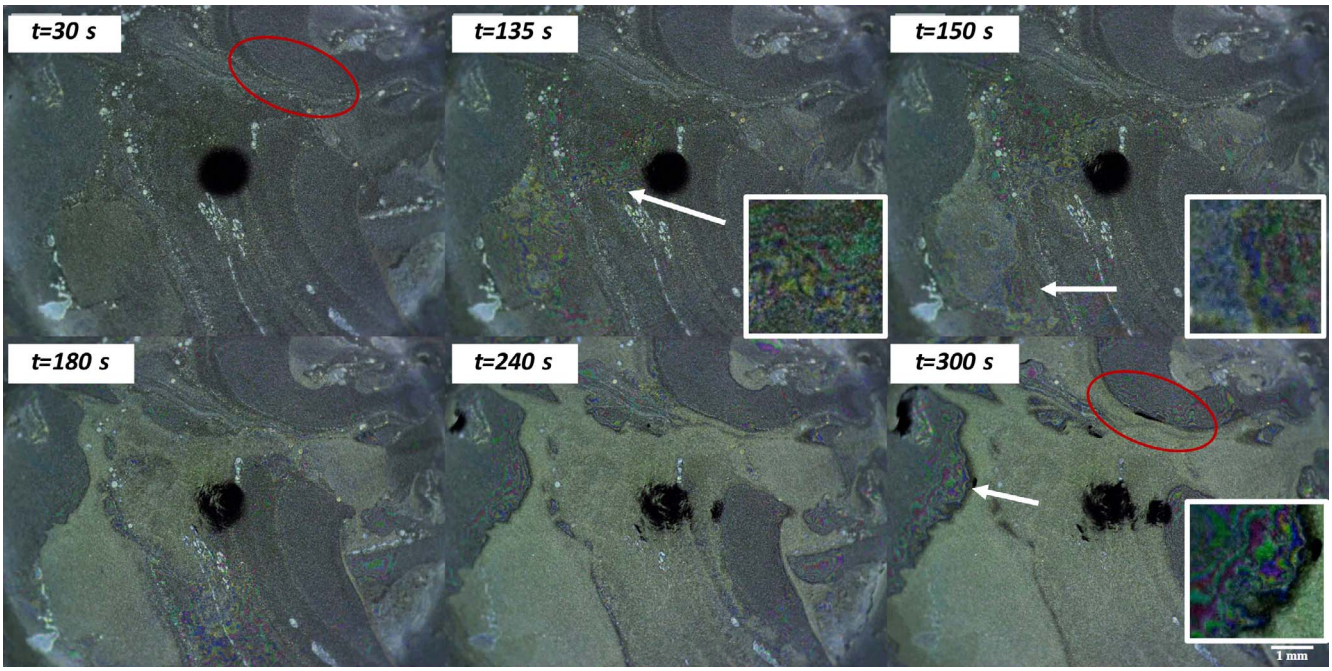

FIGURE 8. Time snapshots of an ATS/meibum film dewetting on a SiHy lens at 35°C. Inserts are zoomed in areas at locations indicated by the white arrows highlighting the appearance of color fringes. The film ATS/meibum dewets through nucleation at multiple sites located all over the lens surface. *Scale*: 1 mm.

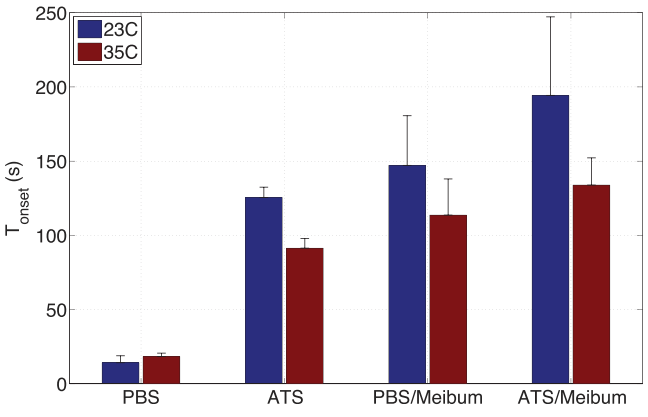

FIGURE 9. Summary of onset of dewetting instability times for model tear films on SiHy lens at 25 and 35°C; T_{onset} is the time for break-up of a film from $t = 0$ of the experiment. Averages and standard deviations are calculated using multiple nucleation site times from three independent trials.

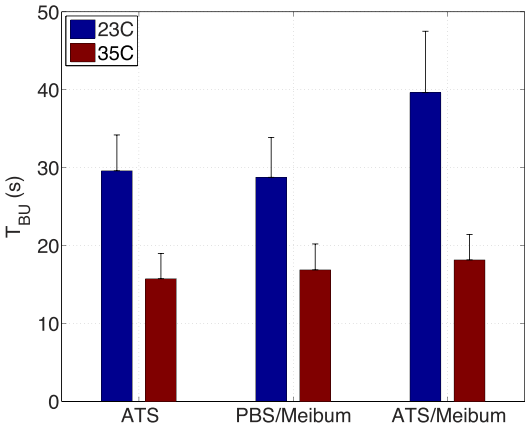

FIGURE 10. Summary of breakup times (T_{BU}) for model tear films on SiHy lens at 25 and 35°C; T_{BU} is the onset of dewetting time calculated from film thickness $h_C = 1.0 \pm 0.3$ μm indicated by the appearance of color fringes. Phosphate buffered saline is not included as it dewets before the appearance of color fringes. Averages and standard deviations are calculated using multiple nucleation sites times from three independent trials.

yield breakup times in the range of 30 to 40 seconds at 23°C. At this temperature, ATS/meibum has a $T_{BU} \sim 40$ seconds; that is greater than both ATS and PBS/meibum, which have $T_{BU} \sim 30$ seconds. In contrast, at the elevated temperature of 35°C, all the three films have $T_{BU} \sim 17 \pm 3$ seconds.

Rate of Evaporation (dh/dt)

A characteristic plot showing the thinning of liquid films as a function of time is shown in Figure 11. This data is fitted to a linear response to obtain the rate of evaporation (dh/dt) and rates for different model tear films are summarized in the Table. The rate of evaporation increases by a factor of 2 for all the films from 0.03 to 0.06 μm/second when the temperature is increased from 23 to 35°C.

DISCUSSION

In this study, we present evidence for the stabilization of model tear films against breakup and dewetting through their interfacial mechanical properties. We thus measure the interfacial shear rheology of our model tear films. We find that pure meibum films (PBS/meibum) exhibit melting characteristics that match past findings.[16] In addition, the ATS films exhibit significant shear moduli that do not diminish significantly with temperature. The surface viscoelastic nature of ATS is attributed to the presence of lysozyme, a globular protein that has been shown to adsorb at the air-liquid interface forming a 2D interfacial gel.[37]

A combination of both ATS and meibum (ATS/meibum) yields higher surface moduli as one may expect. However, the ATS/meibum viscoelasticity does not diminish upon heating, due to competing effects of meibum and proteins at the air-ATS interface. A detailed investigation of the protein-lipid interactions and their physiochemical properties is beyond the scope of this work; however, previous work has indicated that lysozyme can penetrate from the aqueous subphase into the lipid layers and in some cases, increase the elastic properties of the lipid layers.[38,39] It is evident that combining ATS and meibum has a synergistic effect on the surface mechanical properties, leading to higher surface viscoelastic moduli within the measured temperature range.

The onset of dewetting T_{onset} reveals the role of the surface rheology in stabilizing these layers. Dewetting or rupture of the film occurs due to hydrodynamic instabilities once the film has diminished to a critical thickness, and this phenomena has a long history of theoretical and experimental studies.[40] In our experiments, the model tear films drain under the combined influence of gravity and evaporation, until they break up and dewet. Bare PBS films, lacking any protective surface layers, offer poor stability as evidenced through extremely short dewetting times <20 seconds at both 23 and 35°C. Due to the short time-scales for PBS, evaporation does not play a significant role, and the dewetting proceeds by the growth of a single or at most two holes that grow linearly in time as shown in Figure 4.

In contrast to the bare PBS films, the three model tear films, ATS, PBS/meibum, and ATS/meibum have $T_{onset} > 2$ minutes at 23°C. This is expected due to their finite shear moduli, which slows down thinning of the films through the presence of a no-slip boundary condition at the air-liquid interface.[30] Additionally, due to the longer time-scales, evaporation plays a more important role in their dewetting, resulting in dewetting via nucleation and slow growth of a large number of dry patches[31] (see Supplementary Fig. S1). Elevating the temperature to 35°C, leads to a decrease in the T_{onset} by ~30 seconds from their

TABLE. Summary of Measured Parameters for In Vitro Model Tear Films

	PBS		ATS		PBS/Meibum		ATS/Meibum	
	23°C	35°C	23°C	35°C	23°C	35°C	23°C	35°C
T_{onset}, s	14.2 ± 4.7	18.3 ± 2.3	125.5 ± 6.9	91.4 ± 6.4	147.2 ± 33.5	113.7 ± 24.3	194.4 ± 52.9	133.9 ± 18.3
T_{BU}, s	–	–	29.6 ± 4.6	15.7 ± 3.2	28.8 ± 5.1	16.9 ± 3.3	39.6 ± 7.9	18.1 ± 3.3
Rate, μm/s	–	–	0.034 ± .01	0.056 ± .01	0.027 ± .02	0.061 ± .01	0.023 ± .01	0.058 ± .01

Rate of change in film thickness calculated from from initial thickness $h_c \sim 1$ μm. Averages and standard deviations are calculated using multiple nucleation sites times from three independent trials.

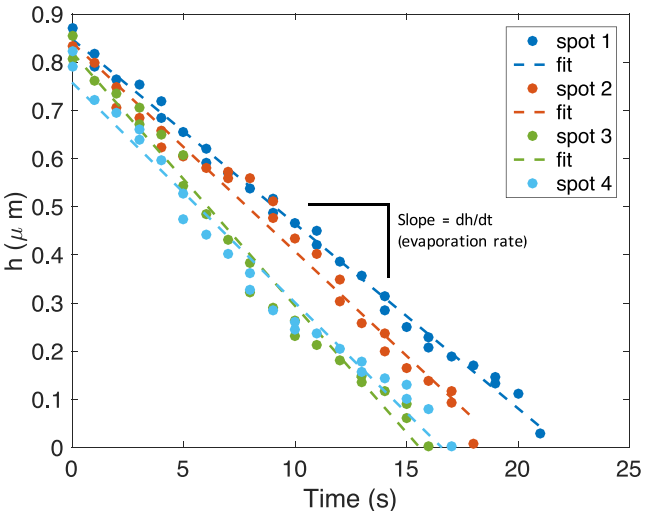

Figure 11. Characteristic curves of film thinning as a function of time for ATS/meibum at 35°C. Multiple spots are evaluated per trial and the data is fit to a linear relationship ($r^2 \geq 0.9$) to estimate the rate of evaporation (dh/dt). A summary of these slopes is provided in the Table.

respective base temperature values, for all three model tear films. The onset times are sensitive to experimental parameters such as temperature, relative humidity, surface pressure, elevation speed, and elevation height. For example, increasing humidity will increase the onset time and postpone dewetting due to a reduced evaporative stress (see Supplementary Fig. S1). Similarly, increasing surface pressure will enhance surface rheology and stabilize the film against breakup (see Supplementary Fig. S2). Additionally, decreasing the elevation speed (from 10 to 0.01 mm/s) results in the coupling of the dewetting process to the elevation dynamics, which has been described in detail previously.[31] For ease of comparison between the model tear films, we keep all parameters constant except for temperature and subphase composition (PBS or ATS).

An interesting result is observed for the PBS/meibum films. At 35°C, meibum melts and the interface is more fluid-like as both $G_s^{'}$ and $G_s^{''}$ plummet by orders of magnitude (Fig. 5). Based on the shear rheology alone, we would expect the T_{onset} of meibum to concomitantly decrease. However, the T_{onset} decreases by only 30 seconds from 147.2 seconds at 23°C to 113.7 seconds at 35°C. One would have expected a larger diminution in T_{onset}, given that the shear viscoelasticity has been significantly reduced. This suggests that shear rheology alone may not be a sufficient index of film stability.

This seemingly discrepant result hints toward the role of the surface dilatational rheology of the meibum layer. The role of both surface shear (μ_s) and dilatational (κ_s) viscosities has been examined in the past in theoretical formulations to predict the stability of thin films by several authors.[41,42] They demonstrated that the films achieve a 4-fold increase in stability as the interface systematically changes from a mobile interface ($\mu_s = \kappa_s = 0$, e.g., water interface) to an immobile interface ($\mu_s, \kappa_s \rightarrow \infty$, e.g., meibomian lipids). A recent contribution from this laboratory also provides experimental evidence that highlights the importance of dilatational viscoelasticity in the stability of lung surfactant films.[43]

The temperature dependence of the dilatational moduli of meibum has been reported by Raju et al.[44] using the oscillating pendant drop method. The outcome of this work reveals two important observations. First, the dilatational elastic and viscous moduli, $E_s^{'} \sim 100$ mN m^{-1} and $E_s^{''} \sim 50$ mN m^{-1}, are an order of magnitude larger than the shear moduli (shown in Fig. 5) at room temperature. Second, upon elevating the temperature to 35°C, the dilatational moduli do not diminish as dramatically as their shear counterparts ($E_s^{'} \sim 40$, $E_s^{''} \sim 20$ mN m^{-1}). Indeed, at physiological temperatures the elastic dilatational modulus remains higher than the viscous dilatational modulus ($E_s^{'} > E_s^{''}$). Finally, comparison of dilatational rheology of healthy and diseased (meibomian gland dysfunction) meibum samples revealed that diseased meibum exhibited predominantly viscous behavior while healthy meibum exhibited primarily elastic properties.[24] Thus, all this evidence suggests that surface dilatational rheology of meibum plays a dominating role in comparison to the surface shear rheology in the stability of the tear film.

It is worth commenting on the correspondence between the onset of breakup times measured here with NI-BUT times that have been previously reported, where interferometry is also employed. By defining $T_{BU} = T_{onset} - T_{fringe}$, we have properly placed the initial condition to correspond to tear film thicknesses normally reported for the PLTF.[34,35] Clinical values of NI-BUT vary depending on the measurement technique: 20.2 ± 5.6 seconds using slit-lamp by Glasson et al.[45] and 11.03 ± 8.6 seconds using interferometry (PLTF thinning time) by Nichols and Sinnott.[2] Our measurements at 23°C reveal T_{BU} ~40 seconds for ATS/meibum and T_{BU} ~30 seconds for both the ATS and PBS/meibum films. The relative value of these times is in correspondence with the relative rheologic properties of these films. At a temperature of 35°C, the T_{BU} for all the three tear films is ~17 ± 3 seconds. These in vitro breakup times are close to the average in vivo values reported by Nichols and Glasson[2] and Glasson et al.[45]

Finally, we discuss the possible effects of evaporation, especially in the final stages of thinning. The change in film height from ~1 μm until zero thickness is surprisingly linear for all the model tears (i.e., nearly constant thinning rates), as seen in a typical data set shown in Figure 11. We find that the rate of thinning or evaporation rate is seemingly unaffected by the presence of meibum: for example, the rate for the artificial tear solution with and without meibum at 35°C is ~4 μm/minutes. These rates are in good agreement with in vivo PLTF thinning rates reported by Nichols et al.[46] This observation is also in agreement with past in vitro experiments that meibum plays a weak role in hindering evaporation. However, a close analysis of the dewetting videos suggests a surprising insight. In Figure 7, the first panel shows the distribution of the lipid layer at 30 seconds, before any breakup, while the last panel shows the remaining lipid at 300 seconds. There is a remarkable correspondence between the features in these two images (red circled areas). Since meibum is highly elastic, there is little movement of the meibum layer during this interval. Thus, it is possible that in some areas where the meibum is thicker, it acts as a better barrier to evaporation. Similar preserved features are also seen in Figure 8 and highlighted. An estimate of the thinning rates in these local spots with thicker meibum yields an average thinning rate between 0.5–1 μm/minute. These results suggest that meibum in vitro can also be an effective barrier to evaporation, at least locally. Thus, our results suggest a dual functionality of meibomian lipids: to stabilize films through their surface dilatational viscoelasticity, as well as reduce evaporation in local areas with richer lipid compositions. However, additional systematic experiments need to be carried out to provide further evidence.

Acknowledgments

The authors thank Patrick Negulescu for help with the interferometry measurements, Yevgenya Strakovsky for contributions to the design of the schematic, and an anonymous reviewer for comments.

Supported by a grant from CooperVision, Inc. (G.G. Fuller).

Disclosure: **M.S. Bhamla**, None; **C. Chai**, None; **N.I. Rabiah**, None; **J.M. Frostad**, None; **G.G. Fuller**, CooperVision, Inc. (F)

References

1. Braun RJ. Dynamics of the tear Film. *Annu Rev Fluid Mech*. 2012; 44:267–297.
2. Nichols JJ, Sinnott LT. Tear film, contact lens, and patient-related factors associated with contact lens-related dry eye. *Invest Ophthalmol Vis Sci*. 2006:47;1319–1328.
3. Sweeney DF, Millar TJ, Raju SR. Tear film stability: a review. *Exp Eye Res*. 2013:117:28–38.
4. Rohit A, Willcox M, Stapleton F. Tear lipid layer and contact lens comfort, eye & contact lens. *Eye Contact Lens*. 2013:39;247–253.
5. Peng CC, Fajardo NP, Razunguzwa T, Radke CJ. In vitro spoilation of silicone-hydrogel soft contact lenses in a model-blink cell. *Optom Vis Sci*. 2015:92;768–780.
6. McMahon TT, Zadnik K. Twenty-five years of contact lenses: the impact on the cornea and ophthalmic practice. *Cornea*. 2000;19; 730–740.
7. Nichols JJ, Ziegler C, Mitchell GL, Nichols KK. Self-reported dry eye disease across refractive modalities. *Invest Ophthalmol Vis Sci*. 2005;46:1911–1914.
8. Faber E, Golding TR, Lowe R, Brennan NA. Effect of hydrogel lens wear on tear film stability. *Optom Vis Sci*. 1991;68:380–384.
9. McCulley JP, Shine WE. Meibomian gland function and the tear lipid layer. *Ocul Surf*. 2003;1:97–106.
10. Mishima S, Maurice DM. The oily layer of the tear film and evaporation from the corneal surface. *Exp Eye Res*. 1961;1:39–45.
11. Craig JP, Tomlinson A. Importance of the lipid layer in human tear film stability and evaporation. *Optom Vis Sci*. 1977;47:8–13.
12. Brown SI, Dervichian DG. The oils of the meibomian glands: physical and surface characteristics. *Arc Ophthalmol*. 1969;82: 537–540.
13. Herok GH, Mudgil P, Millar TJ. The effect of meibomian lipids and tear proteins on evaporation rate under controlled in vitro conditions. *Curr Eye Res*. 2009;34:589–597.
14. Rantamaki AH, Javanainen M, Vattulainen I, Holopainen JM. Do lipids retard the evaporation of the tear fluid? *Invest Ophthalmol Vis Sci*. 2012;53:6442–6447.
15. Cerretani CF, Ho NH, Radke CJ. Water-evaporation reduction by duplex films: application to the human tear film. *Adv Colloic Interface Sci*. 2013;197-198:33–57.
16. Rosenfeld L, Cerretani C, Leiske D, Toney MF, Radke CJ, Fuller GG. Structural and rheological properties of meibomian lipid. *Invest Ophthalmol Vis Sci*. 2013;54:2720–2732.
17. Leiske DL, Miller CE, Rosenfeld L, et al. Molecular structure of interfacial human meibum films. *Langmuir*. 2012;28:11858–11865.
18. Millar TJ, Schuett BS. The real reason for having a meibomian lipid layer covering the outer surface of the tear film - a review. *Exp Eye Res*. 2015;137:125–138.
19. Liang Q, Pan Z, Zhou M, et al. Evaluation of optical coherence tomography meibography in patients with obstructive Meibomian gland dysfunction. *Cornea*. 2015;34:1193–1199.
20. Shimazaki J, Sakata M, Tsubota K. Ocular surface changes and discomfort in patients with meibomian gland dysfunction. *Arch Ophthalmol*. 1995;113:1266–1270.
21. Paugh JR, Knapp LL, Martinson JR, Hom MM. Meibomian therapy in problematic contact lens wear. *Optom Vis Sci*. 1990;67:803–806.
22. Pflugfelder SC, Tseng SC, Sanabria O, et al. Evaluation of subjective assessments and objective diagnostic tests for diagnosing tear-film disorders known to cause ocular irritation. *Cornea*. 1998;17:38–56.
23. Korb DR, Blackie CA. Dry eye is the wrong diagnosis for millions. *Optom Vis Sci*. 2015;92:e350–e354.
24. Georgiev GA, Yokoi N, Ivanova S, Tonchev V, Nencheva Y, Krastev R. Surface relaxations as a tool to distinguish the dynamic interfacial properties of films formed by normal and diseased meibomian lipids. *Soft Matter*. 2014;10:5579–5588.
25. Rosenfeld L, Fuller GG. Consequences of interfacial viscoelasticity on thin film stability. *Langmuir*. 2012;28:14238–14244.
26. Lorentz H, Heynen M, Kay LM, et al. Contact lens physical properties and lipid deposition in a novel characterized artificial tear solution. *Mol Vis*. 2011;17:3392–3405.
27. Roba M, Duncan EG, Hill GA, Spencer ND, Tosatti SGP. friction measurements on contact lenses in their operating environment. *Tribology Lett*. 2011;44:387–397.
28. Nicolaides N, Kaitaranta JK, Rawdah TN, Macy JI, Boswell FM, Smith RE. Meibomian gland studies: comparison of steer and human lipids. *Invest Ophthalmol Vis Sci*. 1981;20:522–536.
29. Leiske D, Monteux C, Senchyna M, Ketelson H, Fuller G. Influence of surface rheology on dynamic wetting of droplets coated with insoluble surfactants. *Soft Matter*. 2011;7:7747–7753.
30. Bhamla MS, Giacomin CE, Balemans C, Fuller GG. Influence of interfacial rheology on drainage from curved surfaces. *Soft Matter*. 2014;10:6917–6925.
31. Bhamla MS, Balemans C, Fuller GG. Dewetting and deposition of thin films with insoluble surfactants from curved silicone hydrogel substrates. *J Colloid Interface Sci*. 2015;449:428–435.
32. Bhamla MS, Nash WL, Elliott S, Fuller GG. Influence of lipid coatings on surface wettability characteristics of silicone hydrogels. *Langmuir*. 2015;31:3820–3828.
33. Yamada M, Mochizuki H, Kawashima M, Hata S. Phospholipids and their degrading enzyme in the tears of soft contact lens wearers. *Cornea*. 2006;25(suppl 1):S68–S72.
34. Nichols JJ, King-Smith PE. Thickness of the pre- and post-contact lens tear film measured in vivo by interferometry, Invest *Ophthalmol Vis Sci*. 2003;44:68–77.
35. Wang J, Fonn D, Simpson TL, Jones L. Precorneal and pre- and postlens tear film thickness measured indirectly with optical coherence tomography. *Invest Ophthalmol Vis Sci*. 2003;44: 2524–2528.
36. Leiske DL, Raju SR, Ketelson HA, Millar TJ, Fuller GG. The interfacial viscoelastic properties and structures of human and animal Meibomian lipids. *Exp Eye Res*. 2010;90:598–604.
37. Freer EM, Yim KS, Fuller GG, Radke CJ. Interfacial rheology of globular and flexible proteins at the hexadecane/water interface: comparison of shear and dilatation deformation. *J Phys Chem B*. 2004;108:3835–3844.
38. Nishimura SY, Magana GM, Ketelson HA, Fuller GG. Effect of lysozyme adsorption on the interfacial rheology of DPPC and cholesteryl myristate films. *Langmuir*. 2008;24:11728–11733.
39. Mudgil P, Torres M, Millar TJ. Adsorption of lysozyme to phospholipid and meibomian lipid monolayer films. *Colloids Surf B Biointerfaces*. 2006;48:128–137.
40. De Gennes P-G, Brochard-Wyart F, Quéré D. *Capillarity and Wetting Phenomena, Drops, Bubbles, Pearls, Waves*. Paris: Springer Science & Business Media; 2004.
41. Narsimhan G, Wang Z. Stability of thin stagnant film on a solid surface with a viscoelastic air-liquid interface. *J Colloid Interface Sci*. 2005;291;296–302.
42. Ruckenstein E, Jain RK. Spontaneous rupture of thin liquid films. *J Chem Society*. 1974;70:132–147.
43. Hermans E, Bhamla MS, Kao P, Fuller GG, Vermant J. Lung surfactants and different contributions to thin film stability. *Soft Matter*. 2015;11:8048–8057.
44. Raju SR, Palaniappan CK, Ketelson HA, Davis JW, Millar TJ. Interfacial dilatational viscoelasticity of human meibomian lipid films. *Curr Eye Res*. 2013;38:817–824.
45. Glasson MJ, Stapleton F, Keay L, Sweeney D, Willcox MD. Differences in clinical parameters and tear film of tolerant and intolerant contact lens wearers. *Invest Ophthalmol Vis Sci*. 2003; 44:5116–5124.
46. Nichols JJ, Mitchell GL, King-Smith PE. Thinning rate of the precorneal and prelens tear films. *Invest Ophthalmol Vis Sci*. 2005;46:2353–2361.

Investigative Ophthalmology & Visual Science